Cisplatinum and Transplatinum Complexes with Benzyliminoether Ligands; Synthesis, Characterization, Structure−Activity Relationships, and In Vitro and In Vivo Antitumor Efficacy

Silvia Mazzega Sbovata,[#] Frazia Bettio,*[,§] Mirto Mozzon,[#] Roberta Bertani,[#] Alfonso Venzo,[†] Franco Benetollo,[‡] Rino A. Michelin,*[,#] Valentina Gandin,[§] and Christine Marzano[§]

Department of Chemical Processes of Engineering, University of Padova, Via F. Marzolo 9, 35131 Padova, Italy, Department of Pharmaceutical Sciences, University of Padova, Via F. Marzolo 5, 35131 Padova, Italy, Institute of Sciences and Molecular Technologies, C.N.R., Via F. Marzolo 1, 35131 Padova, Italy, and ICIS−C.N.R., Corso Stati Uniti 4, 35127 Padova, Italy

Received April 11, 2007

New benzyliminoether derivatives [$PtCl_2${N(H)=C(OMe)CH_2Ph}$_2$] of *cis* (**1a**, **1b**) and *trans* (**2a**, **2b**) geometry were prepared and characterized by means of elemental analysis, multinuclear NMR and FT-IR techniques, and X-ray crystallography; this latter was carried out for **1b**. The cytotoxic properties of these new platinum(II) complexes were evaluated in terms of cell growth inhibition against a panel of different types of human cancer cell lines. *cis*-[$PtCl_2${*E*-N(H)=C(OMe)CH_2Ph}$_2$] (**1a**) was significantly more potent than cisplatin against all tumor cell lines tested, showing IC_{50} values from about 2- to 17-fold lower than the reference compound. Chemosensitivity tests performed on cisplatin-sensitive and -resistant cell lines have demonstrated that complex **1a** is able to overcome cisplatin resistance. Analyzing the mechanism by which complex **1a** led to cell death, we have found that it induced apoptosis in a dose-dependent manner, accompanied by the activation of caspase-3. The in vivo studies carried out using two transplantable tumor models (L1210 leukemia and Lewis lung carcinoma) showed that derivative **1a** induced a remarkable antitumor activity in both tumor models, as measured by prolonged survival and reduced tumor mass compared to control groups.

Introduction

Following the discovery of cisplatin (*cis*-diamminedichloroplatinum(II), *cis*-[$PtCl_2(NH_3)_2$]) and the understanding of its potent anticancer properties in the late 1960s, there has been an explosion of activity aimed at optimizing the antitumor potential of this inorganic coordination complex.[1] Many hundreds of cisplatin (and also transplatin) analogs have been described with the attempt either to reduce the toxic side effects and to circumvent acquired cisplatin resistance.[2−4]

Within this research area, a relevant class of biologically active Pt(II)-based drugs has been prepared from the synthetically useful organonitrile Pt(II) complexes *cis*- and *trans*-[$PtCl_2(NCR)_2$] (R = Me, Ph) by taking advantage of their ability to undergo nucleophilic addition[5,6] of alcohols (R′OH)[7,8] and amines (R′NH_2 and R_2′NH)[9,10] at the C≡N triple bond to obtain iminoether (iminoether = (H)N=C(OR′)R, where R = Me, Ph; R′ = Me, Et) and amidine (amidine = (H)N=C(NHR′)R and (H)N=C(NR_2′)R, where R = Me, Ph; R′ = Me) derivatives, respectively (Scheme 1).

Most of the biological studies reported by Coluccia and Natile have been concerned with the iminoether Pt(II) species.[11] Specifically, *trans*-[$PtCl_2${*E*-(H)N=C(OMe)Me}$_2$], derived by the addition of MeOH to the diacetonitrile complex *trans*-[$PtCl_2(N{\equiv}CMe)_2$],[8] proved to be an excellent antitumor agent, able to overcome cisplatin resistance and displaying a marked intracellular accumulation with respect to cisplatin. Moreover, also the degree of DNA platination was greater for *trans*-platinum iminoether complexes than that of the reference drug, suggesting that DNA is an intracellular target for these compounds.[12] It has also been shown that this new *trans*-compound forms mainly monofunctional adducts at guanine residues on DNA, thus modifying DNA in a different way than cisplatin.[13] In particular, these monofunctional adducts, bending the DNA axis by 21° toward the minor groove, are not recognized by HMGB1 proteins and are readily removed from DNA by nucleotide excision repair. In addition, the most monofunctional adducts readily cross-link proteins, enhancing termination of DNA polymerization.[14]

More recently, we have reported that also Pt(II) amidine complexes of the type *cis*- and *trans*-[$PtCl_2${amidine}$_2$], derived

Scheme 1. Antitumor Platinum(II) Complexes Derived by Nucleophilic Additions of MeOH and Primary ($MeNH_2$) and Secondary Amines (Me_2NH) to Coordinated Organonitriles in *trans*-[$PtCl_2(NCR)_2$] (R = Me, Ph) to Obtain Iminoether (**a**) and Amidine (**b** and **c**) Complexes, Respectively

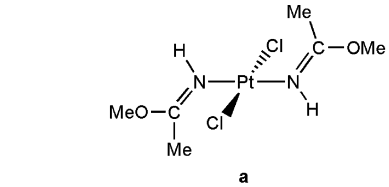

a

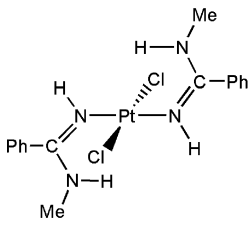

b

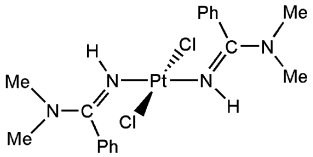

c

* To whom correspondence should be addressed. Phone: +39-049-8275522 (R.A.M.); +39-049-8275365 (F.B.). Fax: +39-049-8275525 (R.A.M.); +39-049-8275366 (F.B.). E-mail: rino.michelin@unipd.it (R.A.M.); frazia.bettio@unipd.it (F.B.).

[#] Department of Chemical Processes of Engineering, University of Padova.

[§] Department of Pharmaceutical Sciences, University of Padova.

[†] Institute of Sciences and Molecular Technologies, C.N.R.

[‡] ICIS−C.N.R.

10.1021/jm070426p CCC: $37.00
Published on Web 08/22/2007

by the addition of primary and secondary amines to the dibenzonitrile complex *cis*- and *trans*-[$PtCl_2(N{\equiv}CPh)_2$], were endowed with significant antitumor activity.[15] It is worthwhile noting that, among this type of complexes, the benzamidine Pt(II) species *trans*-[$PtCl_2\{N(H){=}C(NMe_2)Ph\}_2$] appeared as the most effective derivative in the biological assays. It yielded degrees of cytotoxicity greater (from 2-fold to 9-fold) than cisplatin against various human cancer cell lines and circumvented the acquired cisplatin resistance. The results obtained studying the cellular uptake indicated that the cellular accumulation of *trans*-[$PtCl_2\{N(H){=}C(NMe_2)Ph\}_2$] was about 3-fold higher than that of cisplatin. It has been suggested that the greater biological activity observed, with respect to the reference drug, could be related to the presence of a phenyl ring in the amidine ligand, which likely increases the lipophilicity of the metal complex. Thus, this condition could favor the crossing mechanism through the cell membrane. Moreover, the frequency of DNA−protein cross-links induced by *trans*-[$PtCl_2\{N(H){=}C(NMe_2)Ph\}_2$], being greater than that of cisplatin, might underlie a different mechanism of action from the reference metallodrug.

In view of the above, and to further explore the *cis*/*trans* structure−activity relationship of Pt(II) antitumor complexes, we thought it was interesting to investigate whether the introduction of a phenyl ring into the iminoether ligand structure may have an effect on the biological activity of this class of compounds.

As a part of our investigations aimed at developing new platinum antitumor drugs, this paper describes the synthesis and the spectroscopic and crystallographic characterization of a new class of iminoether derivatives. The in vitro antitumor activity of these new benzyliminoether derivatives against a wide panel of human tumor cell lines, also including different cisplatin-resistant phenotypes, was evaluated. Actually, it is well-known that one of the main goals in the search for new metal-based anticancer agents is the circumvention of the cellular resistance. The inhibition of macromolecular synthesis and the ability to induce apoptosis were investigated to get insight into the mechanism of action of complex **1a**, which was found to be the most effective derivative. Finally, we have investigated the in vivo antitumor activity of **1a** in comparison with cisplatin in two different murine tumor models.

Experimental Section

Instrumental Measurements. IR spectra were recorded on a FT-IR AVATAR 320 of the Nicolet Instrument Corporation (KBr or polyethylene (PE) films) spectrophotometer; the wavenumbers (ν) are given in cm^{-1}. ^1H and ^{13}C NMR spectra were obtained at 298 K as $CDCl_3$ solutions on a Bruker DRX-400 spectrometer operating at 400.13 and 100.61 MHz, respectively, and equipped with a BVT2000 temperature controller. The chemical shift values are given in δ units with reference to internal Me_4Si. Suitable integral values for the proton spectra were obtained by a prescan delay of 10 s to ensure a complete relaxation for all the resonances. The proton assignments were performed by standard chemical shift correlations as well as by 2D correlation spectroscopy (COSY), total correlation spectroscopy (TOCSY), and nuclear overhauser enhancement spectroscopy (NOESY) experiments. The ^{13}C resonances were attributed through 2D-heteronuclear correlation experiments (heteronuclear multiple quantum correlation, HMQC, with bilinear rotation-decoupling, BIRD, sequence[34] and quadrature along F1, achieved using the time-proportional receiver phase incrementation, TPPI, method[35] for the quaternary ones). The elemental analyses were performed by the Microanalysis Laboratory of the Department of Chemical Sciences, University of Padova.

Starting Materials. Solvents were distilled under N_2 prior to use: CH_2Cl_2 and MeOH were distilled from CaH_2, and Et_2O and THF were distilled from sodium benzophenone. Potassium tetrachloroplatinate, K_2PtCl_4, was prepared as described in the literature.[36] Benzylcyanide is a commercially available product from Aldrich and was used as received. Deutherated solvents were purchased from Cambridge Isotope Laboratories (CIL) and were stored under molecular sieves. Transplatin and cisplatin were obtained from Sigma Chemical Co., St. Louis, MO. ^3H-Thymidine (4.77 TBq·mM^{-1}), ^{14}C-thymidine (11 KBq·mM^{-1}), and ^3H-leucine (6.33 TBq·mM^{-1}) were obtained from Amersham International, Inc., U.K. The benzyliminoether complexes **1a** and **2a** were dissolved in DMSO (dimethyl sulfoxide) just before the experiments; calculated amounts of the drug solution were added to the growth medium containing cells to a final solvent concentration of 0.5%, which had no discernible effect on cell killing.

Synthesis of *cis*-[$PtCl_2(NCCH_2Ph)_2$] (1).[37] The compound was prepared by reacting K_2PtCl_4 (2 g, 4.82 mmol) dissolved in deionized water (30 mL) with an excess of $N{\equiv}CCH_2Ph$ (5.6 mL, 48.2 mmol) for 10 days at room temperature. The yellow product was extracted with CH_2Cl_2 (3 × 20 mL), and the solution was dried over anhydrous Na_2SO_4 for 3 h, then filtered off and taken to dryness. Addition of Et_2O (30 mL) gave a yellow solid, which was filtered off and treated with chloroform, which caused only the *trans*-isomer (**2**) to dissolve, while solid *cis*-(**1**) was recovered from the glass frit after washing with Et_2O (3 × 3 mL) and drying under vacuum. Yield 2.08 g (86%). Anal. Calcd ($C_{16}H_{14}Cl_2N_2Pt$): C, 38.41; H, 2.82; N, 5.60. Found: C, 38.25; H, 2.79; N, 5.55. IR (KBr): $\nu_{C{\equiv}N}$ 2318. IR (PE): ν_{Pt-Cl} 358, 348. ^1H NMR ($CDCl_3$): δ 4.17 (s, CH_2, $^3J_{Pt-H}$ = 11.96 Hz), 7.26−7.42 (m, Ph). ^{13}C {^1H} NMR ($CDCl_3$): δ 25.6 (s, *C*H_2, $^3J_{Pt-C}$ = 11.0 Hz), 118.33 (s, *C*≡N, $^2J_{Pt-C}$ = 231.7 Hz), 129.8−130.8 (m, Ph).

Synthesis of *trans*-[$PtCl_2(NCCH_2Ph)_2$] (2).[37] The reaction was carried out as reported for **1** starting from K_2PtCl_4 (2 g, 4.82 mmol) and an excess of $N{\equiv}CCH_2Ph$ (5.6 mL; 48.2 mmol) in deionized water (30 mL) for 3 h at 75 °C. The product, a mixture of *cis*- and *trans*-[$PtCl_2(NCCH_2Ph)_2$], was separated by treatment with chloroform, which dissolves the more soluble *trans*-isomer (**2**). The solution was evaporated under reduced pressure and then treated with Et_2O affording **2** as a yellow solid. Yield 2.13 g (88%). Anal. Calcd ($C_{16}H_{14}Cl_2N_2Pt$): C, 38.41; H, 2.82; N, 5.60. Found: C, 38.29; H, 2.78; N, 5.53. IR (KBr): $\nu_{C{\equiv}N}$ 2318. IR (PE): ν_{Pt-Cl} 342. ^1H NMR ($CDCl_3$): δ 4.22 (s, CH_2, $^3J_{Pt-H}$ = 12.7 Hz), 7.26−7.42 (m, Ph). ^{13}C {^1H} NMR ($CDCl_3$): δ 24.9 (s, *C*H_2, $^3J_{Pt-C}$ = 13.3 Hz), 116.6 (s, *C*≡N, $^2J_{Pt-C}$ = 280.2 Hz), 126.7−129.9 (m, Ph).

Synthesis of *cis*-[$PtCl_2\{Z\text{-}N(H){=}C(OCH_3)CH_2Ph\}_2$] (1b). Complex **1** (0.3 g, 0.6 mmol), dissolved in dichloromethane (5 mL) and methanol (5 mL), was treated with a catalytic amount of KOH (0.02 mmol in 1 mL of methanol). The reaction mixture was stirred for 1 h at room temperature. The solution was then concentrated to a small volume (5 mL) and treated with Et_2O to afford a pale yellow solid. The product was collected and dried under vacuum, affording pure **1b**. Yield 0.12 g (35%). Anal. Calcd ($C_{18}H_{22}Cl_2N_2O_2Pt$): C, 38.31; H, 3.93; N, 4.96. Found: C, 37.98; H, 3.89; N, 4.92. IR (KBr): ν_{N-H} 3226, $\nu_{C=N}$ 1645. IR (PE): ν_{Pt-Cl} 342, 329. ^1H NMR ($CDCl_3$): δ 3.73 (s, CH_2), 4.38 (s, OCH_3), 7.22−7.25 (m, Ph), 8.92 (s, NH). ^{13}C {^1H} NMR ($CDCl_3$): δ 41.90 (s, *C*H_2), 57.63 (s, O*C*H_3), 127.63 (s, Ph, *p-C*), 128.95 (s, Ph, *m-C*), 129.02 (s, Ph, *o-C*), 133.08 (s, Ph, C_1), 175.00 (s, *C*=N). The mother liquor was then concentrated to a small volume and addition of Et_2O gave a mixture of *ZZ*, *ZE*, and *EE* isomers, which were not further purified and characterized. Yield 0.20 g (59%).

Synthesis of *trans*-[$PtCl_2\{Z\text{-}N(H){=}C(OCH_3)CH_2Ph\}_2$] (2b). The reaction was carried out as reported for compound **1b** starting from **2** (0.5 g, 0.99 mmol) dissolved in dichloromethane (5 mL) and methanol (5 mL) and treated with a catalytic amount of KOH (0.03 mmol in 1 mL of methanol). The reaction mixture was stirred for 1 h at room temperature. Yield 0.33 g (60%). Anal. Calcd ($C_{18}H_{22}Cl_2N_2O_2Pt$): C, 38.31; H, 3.93; N, 4.96. Found: C, 37.92; H, 3.87; N, 4.90. IR (KBr): ν_{N-H} 3264, $\nu_{C=N}$ 1646. IR (PE): ν_{Pt-Cl} 304. ^1H NMR ($CDCl_3$): δ 4.88 (s, OCH_3), 3.71 (s, CH_2), 7.33 (s, 1H, Ph, *p-H*), 7.30 (s, 2H, Ph, *m -H*), 7.21 (s, 2H, Ph, *o-H*), 7.50

(s, br, N*H*). ^{13}C {^{1}H} NMR ($CDCl_3$): δ 43.48 (s, *C*H_2), 58.80 (s, O*C*H_3), 127.19 (s, Ph, *p-C*), 128.53 (s, Ph, *m-C*), 129.57 (s, Ph, *o-C*), 134.14 (s, Ph, C_1), 176.0 (s, *C*═N).

Synthesis of *cis*-[$PtCl_2${*E*-N(H)═C(OCH_3)CH_2Ph}$_2$] (1a). Complex **1** (0.3 g, 0.6 mmol) dissolved in dichloromethane (10 mL) and methanol (10 mL) was treated with a catalytic amount of KOH (0.02 mmol in 1 mL of methanol). The reaction mixture was stirred for 1 day at room temperature. The solution was then concentrated to a small volume (5 mL) and treated with Et_2O to afford a yellow solid. The product was collected and dried under vacuum. Yield 0.25 g (74%). Anal. ($C_{18}H_{22}Cl_2N_2O_2Pt$): C, H, N. IR (KBr): ν_{N-H} 3245, $\nu_{C=N}$ 1646. IR (PE): ν_{Pt-Cl} 338, 325. ^{1}H NMR ($CDCl_3$): δ 3.88 (s, O*C*H_3), 4.37 (s, *C*H_2), 7.29 (s, 1H, Ph, *p-H*), 7.31 (s, 2H, Ph, *m-H*), 7.29 (s, 2H, Ph, *o-H*), 8.27 (s, NH). ^{13}C {^{1}H} NMR ($CDCl_3$): δ 41.67 (s, *C*H_2), 57.12 (s, O*C*H_3), 127.67 (s, Ph, *p-C*), 128.99 (s, Ph, *m-C*), 129.69 (s, Ph, *o-C*), 134.10 (s, Ph, C_1), 173.26 (s, *C*═N).

Synthesis of *trans*-[$PtCl_2${*E*-N(H)═C(OCH_3)CH_2Ph}$_2$] (2a). The reaction was carried out as reported for compound **1a** starting from **2** (0.5 g, 0.99 mmol) dissolved in dichloromethane (10 mL) and methanol (10 mL) and treated with a catalytic amount of KOH (0.03 mmol in 1 mL of methanol). The reaction mixture was stirred for 1 day at room temperature. Yield 0.45 g (80%). Anal. ($C_{18}H_{22}Cl_2N_2O_2Pt$): C, H, N. IR (KBr): ν_{N-H} 3222, $\nu_{C=N}$ 1639. IR (PE): ν_{Pt-Cl} 304.7. ^{1}H NMR ($CDCl_3$): δ 3.80 (s, O*C*H_3), 4.53 (s, *C*H_2), 7.23 (s, 1H, Ph, *p-H*), 7.28 (s, 2H, Ph, *m-H*), 7.51 (s, 2H, Ph, *o-H*), 8.05 (s, br, N*H*). ^{13}C {^{1}H} NMR ($CDCl_3$): δ 41.50 (s, *C*H_2), 55.60 (s, O*C*H_3), 127.19 (s, Ph, *p-C*), 128.53 (s, Ph, *m-C*), 129.57 (s, Ph, *o-C*), 134.14 (s, Ph, C_1), 171.95 (s, *C*═N).

Molar Conductivity. The molar conductivity values for **1a**, **2a**, cisplatin, and transplatin were determined using Crisom 522 digital conductimeter, available at the Department of Chemical Science, University of Padova. The compounds were dissolved in DMSO, and the measurements were done at the following concentrations: 0.05 mM, 0.2 mM, 0.5 mM, 1.25 mM, and 2.5 mM. The molar conductivity (Λ_m) was calculated as $\Lambda_m = k/c$, where k is the specific conductivity and c is the concentration.[38] The molar conductivity values were plotted against concentration, and the curve was extrapolated to zero concentration to obtain the limiting value.

X-ray Crystallography. Crystal data for complex **1b**·MeOH: $C_{19}H_{26}N_2O_3Cl_2Pt$, Mr 596.41, triclinic space group $P\bar{1}$, a = 9.813(2), b = 11.532(3), c = 10.847(3) Å, α = 66.59(2), β = 92.16(3), γ = 105.10(3)°, V = 1084.6(5) Å^3, Z = 2, ρ_{calcd} = 1.823 g cm^{-3}, Mo Kα radiation (λ = 0.71073 Å); μ = 6.735 mm^{-1}, F(000) 578.

A pale yellow crystal of compound **1b**·MeOH obtained by recrystallization from CH_2Cl_2/MeOH/Et_2O was lodged in Lindemann glass capillary and centered on a four circle Philips PW1100 diffractometer using graphite monochromated Mo Kα radiation (0.710 73 Å), following the standard procedures at room temperature. All intensities were corrected for Lorentz polarization and absorption.[39] The structures were solved by the heavy-atom method[40] and were refined by full-matrix least-squares procedures (based on F_o^2) using anisotropic temperature factors for all nonhydrogen atoms. Hydrogen atoms were introduced at calculated positions in their described geometries and during refinement were allowed to ride on the attached carbon atoms with fixed isotropic thermal parameters (1.2 U_{equiv} of the parent carbon atom). Final agreement factors $wR' = [\Sigma w(F_o^2 - F_c^2)^2/\Sigma w(F_o^2)^2]^{1/2} = 0.076$, $S = 1.152$, and conventional $R = 0.029$, based on the F values of 4582 reflections having $I = 2\sigma(I)$. Structure refinement and final geometrical calculations were carried out with the SHELXL-97[41] program, implemented in the WinGX package.[42]

Cell Cultures. HeLa, A549, CaCo-2, MCF7, and HepG2 are human cervix, lung, colon, breast, and hepatocellular carcinoma cell lines, respectively, which were obtained from ATCC (Rockvill, MD), along with the malignant melanoma (A375) and human promyelocytic leukemia (HL60). Human ovarian cancer cell line (2008) and its cisplatin-resistant variant, C13* cells, were kindly provided by Prof. G. Marverti (Department of Biomedical Science of Modena University, Italy). A431 human cervix carcinoma and U2OS human osteosarcoma cell lines were kindly provided by Prof. Zunino (Division of Experimental Oncology B, Istituto Nazionale dei Tumori, Milan, Italy), along with the cisplatin-resistant counterparts, A431/Pt and U2OS/Pt cells. All cisplatin-resistant sublines were selected after continuous in vitro exposure to increasing concentration of cisplatin.[25−27] Murine leukaemia cisplatin-sensitive L1210 and -resistant L1210/R cells were harvested from the peritoneal cavity of the tumor bearing BALB/c × DBA/2 F_1 mice 10 days after transplantation (see In Vivo Studies).

Cell lines were maintained in the logarithmic phase at 37 °C in a 5% carbon dioxide atmosphere using the following culture media: (i) RPMI-1640 medium (Euroclone, Celbio, Milan, Italy), containing 10% foetal calf serum (Biochrom-Seromed GmbH&Co, Berlin, Germany) and supplemented with 25 mM HEPES buffer, with L-glutamine, and with antibiotics penicillin (50 units·mL^{-1}) and streptomycin (50 μg·mL^{-1}) for MCF7, HL60, 2008, C13*, A431, A431/Pt cells, L1210, and L1210/R; (ii) McCoy's (Euroclone, Celbio, Milan, Italy) medium, supplemented with 10% foetal calf serum (Euroclone, Celbio, Milan, Italy), 0.1% gentamicin for U2OS and U2OS/Pt cells; (iii) D-MEM (Dulbecco's modified eagle's) medium (Euroclone, Celbio, Milan, Italy), supplemented with 10% foetal calf serum (Euroclone, Celbio, Milan, Italy), penicillin (50 units·mL^{-1}), and streptomycin (50 μg·mL^{-1}) for A375 and A549 cells; (iv) MEM (minimum essential Eagle's) medium (Euroclone, Celbio, Milan, Italy), supplemented with 10% foetal calf serum (Euroclone, Celbio, Milan, Italy), penicillin (50 units mL^{-1}), and streptomycin (50 μg·mL^{-1}) for HepG2 and CaCo-2 cells; (v) F-12 HAM'S (Sigma Chemical Co.), containing 10% foetal calf serum, L-glutamine, penicillin (50 units·mL^{-1}), and streptomycin (50 μg·mL^{-1}) for HeLa cells.

Cytotoxicity Assay. The growth inhibitory effect toward tumor cell lines was evaluated by means of MTT (tetrazolium salt reduction) assay.[43] Briefly, between 3 and 8 × 10^3 cells, dependent upon the growth characteristics of the cell line, were seeded in 96-well microplates in growth medium (100 μL) and then incubated at 37 °C in a 5% carbon dioxide atmosphere. After 24 h, the medium was removed and replaced with a fresh one containing the compound to be studied at the appropriate concentration. Triplicate cultures were established for each treatment. After 48 h, each well was treated with 10 μL of a 5 mg·mL^{-1} MTT (3-(4,5-dimethylthiazol-2-yl)-2,5-diphenyltetrazolium bromide) saline solution, and after 5 h of incubation, 100 μL of a sodium dodecylsulfate (SDS) solution in HCl (0.01 M) was added. After overnight incubation, the inhibition of cell growth induced by tested compounds was detected by measuring the absorbance of each well at 570 nm using a Bio-Rad 680 microplate reader (Milan, Italy). Mean absorbance for each drug dose was expressed as a percentage of the control untreated well absorbance and plotted vs drug concentration. IC_{50} values represent the drug concentrations that reduced the mean absorbance at 570 nm to 50% of those in the untreated control wells.

Inhibition of Macromolecular Synthesis. A total of 4 × 10^5 cells·mL^{-1} 2008 were seeded in 60 mm Petri dishes in RPMI-1640 growth medium (5 mL). After 24 h, the medium was removed and replaced by a fresh one containing the compound to be studied, previously dissolved in the minimum required quantity of DMSO (to a final organic solvent concentration of 0.5% (v/v)) at the appropriate concentration; cells were then incubated for 3 h at 37 °C in a 5% carbon dioxide atmosphere. Triplicate cultures were established for each treatment. Hence, the cells were centrifuged, and the harvested precipitate was resuspended in an aqueous solution constituted by 0.5 mL of PBS solution, 0.1 mL of physiological solution, and 35−40 KBq of tritiated thymidine, uridine, or leucine and reincubated for 30 min at 37 °C. The labeling reaction was stopped by cooling in ice and adding 1 mL of a 5 mM solution of unlabeled precursor in physiological solution. Cells were then harvested by filtration through a Whatman GF/C glass microfibre filter (1.2 μm), washed three times with cold PBS solution, and treated with 5 mL of 5% trichloroacetic acid solution. After 3 min, the samples were filtered again, washed several times with 10 mL of 1% trichloroacetic acid solution, and air-dried at

room temperature. Radioactivity of the acid-precipitable fraction was determined by dipping the dried filters into 5 mL of a toluene-base scintillator (5 g of 2,5-diphenyloxazole, 0.25 g of 1,4-bis(4-methyl-5-phenyloxazol-2-yl)benzene, and toluene addition up to 1 L of solution) and using a liquid scintillation TriCarb 1900TR counter. The results were calculated as the percentage of radioactivity incorporated into the DNA with respect to untreated control cells.

Induction of Apoptosis. Caspase-3 activity was detected by using the ApoAlert Caspase-3 Fluorescent Assay Kit (Clontech) according to the manufacturer recommended procedures. In the amount of 10^6 2008 cells were collected following 24 h of incubation of tested compounds (at concentrations corresponding to IC_{50} values) and lysed on ice in 50 μL of lysis buffer for 10 min and then treated with 50 μL of reaction buffer containing dithiothreitol (DTT) and 5 μL of caspase-3 substrate solution (Asp-Glu-Val-Asp-7-amino-4-trifluoromethyl-coumarin [DEVD-AFC], Clontech). The fluorescence was determined with a Perkin-Elmer 550 spectrofluorometer (excitation 440 nm, emission 505 nm). The caspase-3 activity was expressed as the increase of the AFC-emitted fluorescence. The Student's t-test was used for data analysis.

In Vivo Studies. All of the animal experiments were carried out in accordance with the Guide for the Care and Use of Laboratory Animals, as adopted and promulgated by the NIH. All the animals were allowed food and water ad libitum.

Acute toxicity studies were performed in BALB/c mice (Charles River, Italy), both male and female, in groups of 10 animals per dose. The tested compounds, at different concentrations, were injected i.p. one time, and animal weight and survival were observed for 1 month.

The L1210 leukaemia and Lewis lung carcinoma lines were obtained as frozen stock from NCI (National Cancer Institute, U.S.A.) and maintained in DBA/2 and C57BL/6 syngenic mice, respectively (Charles River, Italy). L1210/R, a cisplatin-resistant subline of L1210, was established in this institute by intraperitoneal treatment of a single dose of cisplatin (6−8 mg·kg^{-1}) administered 2 days after the passage of 10^6 L1210 cells over successive generations in BALB/c × DBA/2 F_1 mice.[28]

For in vivo antitumor activity studies against mouse leukaemia L1210 and L1210/R 6 weeks aged BALB/c × DBA/2 F_1 mice (18 ± 2 g body weight, 8 mice/group, 10 controls) were inoculated i.p. with 1×10^5 cells/0.1 mL/mouse on day 0. Test compounds, freshly dissolved in DMSO, were administrated i.p. on days 1, 5, and 9 (2.5−10 mg·kg^{-1} for **1a** complex, 1 mg × kg^{-1} for cisplatin) after tumor implantation. The in vivo antitumor activity was evaluated by comparing the mean survival time of treated groups (*T*) with that of control groups (*C*) and was expressed by percentage value of *T*/*C* (%*T*/*C*).

Lewis lung carcinoma was implanted i.m. as a 2×10^6 cells inoculum into the right hind leg of C57BL/6 mice (24 ± 3 g body weight, 8 animals/ group, 10 controls). The treatment with tested drugs began 24 h after implant and was performed i.p. from day 1 to day 6 in 10% DMSO/90% PBS at its predetermined nontoxic dose (2.5−10 mg·kg^{-1} for **1a** complex, 1 mg·kg^{-1} for cisplatin). At day 11 animals were sacrificed, the legs were amputated at the proximal end of the femur, and the inhibition of tumor growth was determined according to the difference in weight of the tumor-bearing leg and the healthy leg of the animals expressed as % referred to the control animals.

Results and Discussion

Synthesis and Characterization of the Complexes. As mentioned in the Introduction, the addition of alcohols (R′OH) to nitriles (NCR) coordinated to platinum(II) takes places readily in the presence of a catalytic amount of a base. As previously reported by Natile et al.,[7,8] the iminoether ligand formed can have either *E* or *Z* configuration at the C═N double bond, corresponding to a *cis*- or *trans*-addition of the alcohol to the C≡N triple bond, respectively.

Scheme 2. Synthesis of the Benzyl−Iminoether Complexes with *E*-Configuration

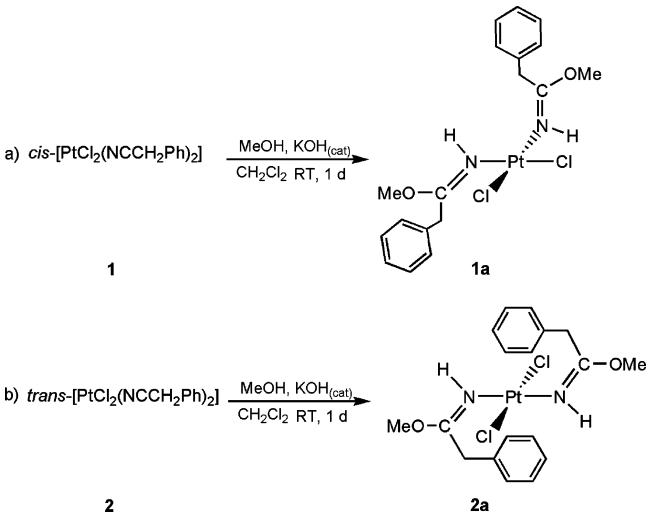

Scheme 3. Synthesis of the Benzyl−Iminoether Complexes with *Z*-Configuration

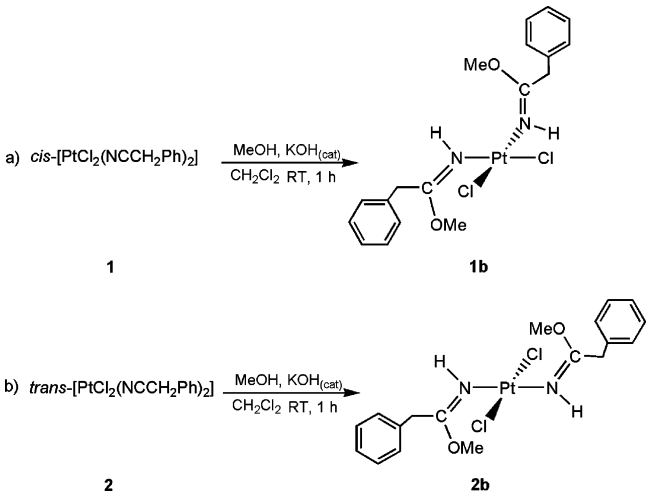

Complexes **1** and **2** (Scheme 2), dissolved in a mixture of dichloromethane/methanol (1:1, v/v) and in the presence of a catalytic amount of KOH, undergo, at room temperature, nucleophilic addition of MeOH, affording (after 24 h) the diiminoether derivatives *cis*- and *trans*-[$PtCl_2${*E*-N(H)═C(OMe)-CH_2Ph}$_2$] (**1a**, **2a**; Scheme 2a,b), where both ligands are in the *E* configuration.

The reaction of complexes **1** and **2** with MeOH, performed in shorter reaction times and with a higher concentration of reactants, leads to the isolation of complexes **1b** and **2b**, respectively, bearing the two iminoether ligands in the *Z* configuration (Scheme 3).

Once isolated, complexes **1b** and **2b**, which are the kinetically favored species, are stable in the solid state and in an organic solvent solution, but they undergo isomerization into the thermodynamically more stable isomers **1a** and **2a**, respectively, in the presence of a small amount of base (KOH). The $Z \rightarrow E$ isomerization process has been described in detail by Natile and co-workers[8] for similar compounds.

Compounds **1a**, **2a**, **1b**, and **2b** were characterized by microanalysis, IR, and ^{1}H and ^{13}C NMR spectroscopy (see also Experimental Section), and **1b** was also characterized by X-ray diffraction (see later). The IR spectra (KBr) show the N−H stretching band in the range 3222−3264 cm^{-1}, while the C═N

Table 1. Selected ^{1}H NMR and ^{13}C NMR Data for Compounds **1a, 2a, 1b, and 2b**

	^{1}H NMR[a]			^{13}C{^{1}H} NMR[a]		
cmpd	δ_{N-H}	$\delta_{CH_2-C=N}$	$\delta_{(OCH_3)C=N}$	$\delta_{CH_2-C=N}$	$\delta_{(OCH_3)-C=N}$	$\delta_{R-C=N}$
1a	8.27	4.37	3.88	41.67	57.12	173.26
2a	8.05	4.53	3.80	41.50	55.60	171.95
1b	8.92	3.73	4.38	41.90	57.63	175.00
2b	7.50	3.71	4.88	43.48	58.80	176.00

[a] The spectra were recorded in $CDCl_3$; δ in ppm, rt.

vibration appears in the range 1639−1646 cm^{-1}. The Pt−Cl absorptions are found in the expected range of 305−342 cm^{-1}.[16] Selected ^{1}H NMR and ^{13}C NMR data, in $CDCl_3$, for these complexes are collected in Table 1.

The *E* or *Z* conformation of the iminoether ligand can be readily inferred by the ^{1}H NMR data upon observing the position of the chemical shifts of the methylene and the methoxy groups because a downfield shift is expected for the protons that come close to platinum,[8,17] that is, the CH_2 protons in the *E* configuration and the OCH_3 protons in the *Z* configuration. In particular, we observed that for the *E* configuration the methoxy group displays a singlet resonance at δ 3.80 and δ 3.88 for **1a** and **2a**, respectively, and that corresponding to the CH_2 group is observed at δ 4.37 and δ 4.53 for **1a** and **2a**, respectively. For the *Z* species, this trend is reversed, that is, the CH_2 resonances are shown up at δ 4.38 and δ 4.88 for **1b** and **2b**, respectively, while the OCH_3 resonances are shifted to δ 3.73 and δ 3.71, respectively.

The *E* and *Z* configuration of the iminoether ligands is further confirmed by NOESY experiments by the observation of the Overhauser dipolar correlation between the C*H*$_2$, OC*H*$_3$, and N*H* signals. In the case of the ligands in the *E* configuration, the NOESY maps display correlations between the Pt−NH and OCH_3 proton signals; while, in the case of the *Z*-isomers, correlations between the Pt−NH and the CH_2 proton signals are detected. The proton NMR spectra of *trans*-isomers either in the *Z* or the *E* configuration exhibit signals of the aromatic protons in the range δ 7.20−7.51, clearly showing an interaction between the phenyl ring and the metal. In particular, the *ortho*-protons of **2a** are shifted downfield due to their position with respect to the platinum center.[17c] The conformation of **2b** reported in Scheme 3 is supported also by dipolar correlations between the OCH_3 and the *ortho*-phenyl protons, which are absent in the case of **2a**. In the ^{1}H NMR spectra of the *cis*-isomers **1a** and **1b**, the aromatic protons show quite similar chemical shift values, giving rise to largely overlapping signals. The presence in the NOESY maps of correlations between the OCH_3 and the *ortho*-protons support the conformations reported in Schemes 2 and 3.

It is known that the chloride substitution process at the platinum coordination sphere is usually considered to be a necessary prelude to biological activity.[18] Preliminary results indicated that the two complexes **1a** and **2a** show a markedly different conductivity behavior in DMSO, the solvent used in the biological assays, while complexes **1b** and **2b** were not studied owing to their poor solubility (see below). The molar conductivity of a series of DMSO solutions at different concentrations was determined for compounds **1a**, **2a**, cisplatin, and transplatin. The limiting values of molar conductivity (in ohm^{-1} cm^2 mol^{-1}) at zero concentration of **1a** and cisplatin are 33 and 34, respectively. While the limiting values of molar conductivity (in ohm^{-1} cm^2 mol^{-1}) of **2a** was found to be 18 (44 for transplatin), all of these values fall in the range expected for 1:1 electrolytes in DMSO.[19]

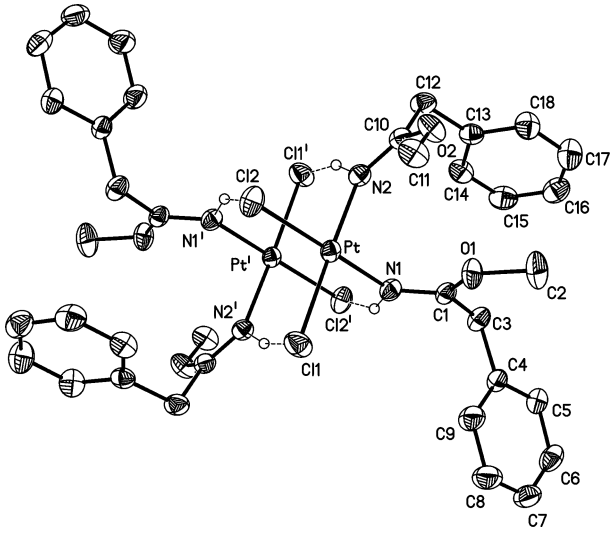

Figure 1. Perspective ORTEP drawing of a "dimer" of **1b** with the atom-labeling scheme. H atoms involved in the N−H···Cl bridges were set in calculated positions (' at -x, -y, 1-z). Selected bond lengths (Å) and angles (°): Pt−N(1) 1.991(4), Pt−N(2) 2.022(4), Pt−Cl(1) 2.303(2), Pt−Cl(2) 2.307(2), N(1)−C(1) 1.281(6), C(1)−O(1) 1.320(6), C(1)−C(3) 1.499(7), Pt···Pt′ 3.457(1); Cl(1)−Pt−Cl(2) 91.8(1), N(1)−Pt−N(2) 86.7(2), Cl(1)−Pt−N(1) 89.9(1), Cl(1)−Pt−N(2) 176.0(1), Cl(2)−Pt−N(2) 91.4(1), Cl(2)−Pt−N(1) 174.5(1), N(1)−C(1)−O(1) 116.2(5), Cl−H···N average 153.

X-ray Diffraction Study of 1b. The ORTEP drawing of **1b** is reported in Figure 1 together with selected bond distances and angles.

The structure of the complex consists of one "dimer" {$Pt_2Cl_4L_4$} (L = iminoether ligand) formed by two $PtCl_2L_2$ units intermoleculary held together by four N−H···Cl hydrogen bonds (H···Cl 2.58 Å) involving the chlorines and the iminoetheric protons of the centro-symmetrically related molecules. The Pt···Pt′ contact distance of 3.457(1) Å is not short enough for a metal−metal interaction, but is a consequence of the hydrogen bond intermolecular interactions which determine the dimer formation. A similar feature was previously observed in the crystal structure of the bis-amidine complexes *cis*-[$PtCl_2${*E*-N(H)=C(NMe$_2$)Me}$_2$][10a] and *trans*-[$PtCl_2${N(H)=C(NCH$_2$CH$_2$)Ph}$_2$],[20] where two $PtCl_2L_2$ units are associated through four N−H···Cl hydrogen bonds (H···Cl average 2.6 Å and 2.4 Å, respectively) with Pt···Pt contact distances of 3.469(1) Å and 3.443(5) Å, respectively.

The square planar geometry around the metal is characterized by *cis*-position of the ligands. The two iminoether molecules have the *Z* configuration and similar geometric parameters, but a slightly different shape to bring one OMe group toward the phenyl ring of the iminoether in *cis*-position (with a Cl(1)−O(1) contact of 2.565 Å).

Biological Activity. Cytotoxicity on Human Cancer Cells. *cis*- and *trans*-Benzyliminoether derivatives **1a** and **2a**, were evaluated for their cytotoxic properties against a panel of human tumor cell lines containing examples of cervix (HeLa), breast (MCF7), lung (A549), colon (Caco-2), and hepatocellular (HepG2) cancer, leukaemia (HL60), and melanoma (A375). For comparison purposes, the cytotoxicities of transplatin and cisplatin were examined under the same experimental conditions. *cis*- and *trans*-Isomers having a *ZZ* configuration (**1b** and **2b**) were much less soluble in common solvents and their solubility was not sufficient for biological testing, as also previously observed for a similar compound, that is, *trans*-[$PtCl_2${*Z*-N(H)=C(OCH$_3$)CH$_3$}$_2$], by Coluccia and co-workers.[21]

Table 2. Cytotoxic Activity[a]

	IC_{50}[b] (μM) ± S.D.[c]						
cmpd	HeLa	MCF-7	A375	A549	Caco-2	HepG2	HL60
1a	3.01 ± 0.4	19.11 ± 1.3	9.15 ± 1.2	2.33 ± 1.7	5.37 ± 1.4	7.05 ± 1.2	8.59 ± 2.7
2a	65.32 ± 2.0	68.12 ± 1.0	77.55 ± 1.8	87.90 ± 2.6	80.12 ± 2.3	79.21 ± 2.5	89.98 ± 1.2
cisplatin	11.75 ± 1.5	30.18 ± 1.5	20.28 ± 1.3	39.27 ± 1.9	35.37 ± 1.4	21.54 ± 1.3	18.35 ± 1.6
transplatin	>100	>100	>100	>100	>100	>100	>100

[a] Cells ($3-8 \times 10^4$ mL^{-1}) were treated for 48 h with increasing concentrations of the tested compounds. Cytotoxicity was assessed by MTT test. [b] IC_{50} values were calculated by probit analysis ($P < 0.05$, χ^2 test). [c] S.D. = standard deviation.

Table 3. Cross-Resistance Profiles[a]

	IC_{50}[b] ± S.D.[c] (μM)							
cmpd	2008	C13*	A431	A431/Pt	U2OS	U2OS/Pt	L1210	L1210/Pt
1a	5.45 ± 2.7	11.48 ± 2.1 (2.1)	9.12 ± 2.3	8.58 ± 2.4 (0.9)	1.66 ± 0.1	3.31 ± 2.5 (1.9)	6.07 ± 1.0	8.49 ± 1.1 (1.4)
2a	83.34 ± 1.2	>100	>100	90.03 ± 1.2	87.2 ± 2.1	>100	97.09 ± 2.5	>100
cisplatin	12.69 ± 1.7	89.18 ± 4.5 (7.0)	22.06 ± 2.1	57.76 ± 1.8 (2.6)	20.16 ± 6.8	75.88 ± 1.7 (3.8)	2.14 ± 1.7	64.89 ± 4.5 (30.3)
transplatin	>100	>100	>100	>100	>100	>100	>100	>100

[a] The numbers in parentheses are the values for RF (resistance factor) = (IC_{50} − resistant cell line)/(IC_{50} − parent cell line). [b] IC_{50} values were calculated by probit analysis ($P < 0.05$, χ^2 test). Cells ($3-8 \cdot 10^4 \cdot$mL^{-1}) were treated for 48 h with increasing concentrations of the tested compounds. Cytotoxicity was assessed by MTT test. [c] S.D. = standard deviation.

IC_{50} values, calculated from the dose−survival curves obtained after 48 h of drug treatment by the MTT test, are shown in Table 2.

Similarly to transplatin, which was found to be scarcely effective, the *trans*-isomer (**2a**) showed a negligible activity in all cancer cell lines. On the contrary, the *cis*-isomer (**1a**) showed a growth inhibitory potency markedly higher than that of cisplatin. In particular, in HepG2 and HeLa cells, the obtained IC_{50} values were about 3 and 4 times lower than those calculated for cisplatin, respectively.

Moreover, in Caco-2 colon cancer cells, intrinsically resistant to cisplatin,[22] and A549 non-small lung adenocarcinoma cells, with notoriously poor chemosensitivity to cisplatin,[23] complex **1a** cytotoxicity exceeded that of the reference metallodrug by a factor of about 8 and 16, respectively, thus indicating that **1a** is able to circumvent intrinsic resistance to cisplatin.

It is worthwhile noting that the complex **1a** represents the first example of an iminoether derivative, having *cis*-geometry, endowed with a marked cytotoxic potency.[12a,21,24]

The interesting results that we have obtained against the in-house panel of human tumor cell lines, prompted us to test the cytotoxic activity of the new benzyliminoether derivatives onto additional human cell line pairs selected for their resistance to cisplatin after in vitro exposure to an increasing concentration of cisplatin: 2008/C13* (human ovarian carcinoma),[25] A431/A431-Pt (human squamous cervix carcinoma),[26] U2OS/U2OS-Pt (human osteosarcoma).[27] Although cisplatin resistance is multifactorial, the main molecular mechanisms involved in resistance in these sublines have almost been defined. In C13* cells, resistance is correlated to reduced cellular drug uptake, high cellular glutathione levels, and enhanced repair of DNA damage.[25] In human squamous cervix carcinoma A431-Pt cells, resistance is due to a defect in drug uptake and to decreased levels of proteins involved in DNA mismatch repair (MSH2), causing an increased tolerance to cisplatin-induced DNA damage.[26] In osteosarcoma U2OS-Pt cells, an analysis of their phenotype indicated that resistance is associated to a reduced drug uptake, to a reduced formation of DNA lesions and to a defect in the DNA mismatch repair and upregulation of β-DNA polymerase.[27]

Chemosensitivity tests were also carried out on cells that had acquired resistance to cisplatin in vivo. L1210-R murine leukaemia cells were developed by treatment of L1210-bearing mice with a single dose of cisplatin according to the literature procedure.[28]

Cytotoxicity of tested complexes in sensitive and resistant cells were assessed after a 48 h drug exposure by MTT test; for comparison purposes, the cytotoxicity of cisplatin was also evaluated under the same experimental conditions. Cross-resistance profiles were evaluated by means of the resistance factor (RF), which is defined as the ratio between IC_{50} values calculated for the resistance cells and those arising from the sensitive ones (Table 3).

While transplatin and complex **2a** proved to be quite ineffective in all cell line pairs, complex **1a** appeared to be much more cytotoxic than cisplatin on both cisplatin-sensitive and -resistant sublines. In fact, against the ovarian, cervix cancer, and osteosarcoma, RF values were about 4, 3, and 2 times lower than those calculated for cisplatin, respectively. With regard to murine leukaemia cell line pairs, L1210/R cells were shown to be about 30-fold more resistant to cisplatin than were the parental L1210 cells. Noticeably, complex **1a** showed an almost equal growth inhibitory effect on both the original and the resistant L1210/R cells, displaying an RF value about 22 times lower than that calculated for cisplatin. These results, confirming the circumvention of cisplatin resistance by complex **1a**, are particularly interesting as L1210-R cells, in respect to the resistant sublines previously mentioned, had acquired their resistance in vivo, thus evading all the host defense mechanisms.

The overcoming of cross-resistance phenomena in all cell line pairs supports the hypothesis of a different pathway of action of this benzyliminoether platinum complex than that of cisplatin. In particular, the cellular response of A431/Pt and U2OS/Pt cells might be consistent with the formations of different types of DNA lesions, as compared to cisplatin, or less efficiently repaired by DNA mismatch repair systems.[27] Moreover, by virtue of a possible enhanced lipophilicity due to the presence of the phenyl ring in the iminoether structure, the complex **1a** could enter resistant cells with a kinetic uptake very similar to that achieved in parental cell lines. The results obtained with C13* cells strongly support its ability to overcome the modifications in the plasma membrane belonging to resistant cells and responsible for a reduced cisplatin accumulation.[25]

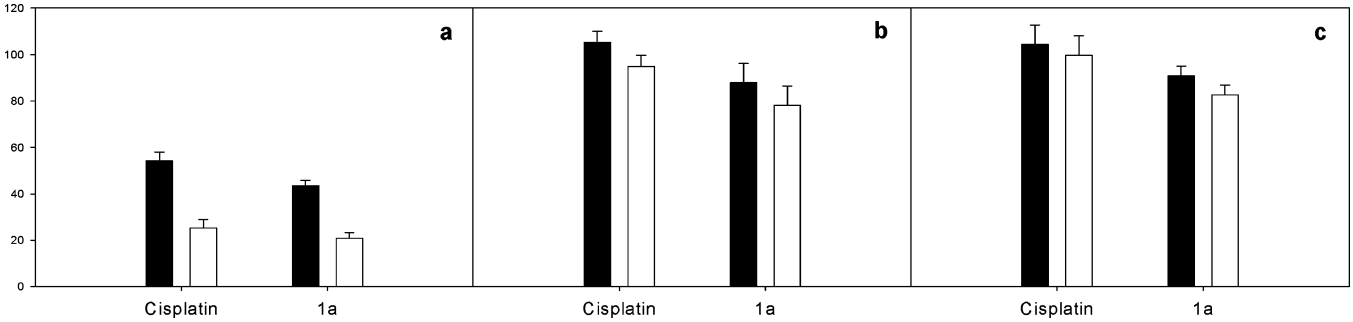

Figure 2. Macromolecular synthesis inhibition in 2008 cells treated for 3 h with 12 μM (□) and 25 μM (■) of complex **1a** or cisplatin. Bars represent the corresponding standard deviations: (a) inhibition of DNA synthesis; (b) inhibition of RNA synthesis; and (c) inhibition of protein synthesis.

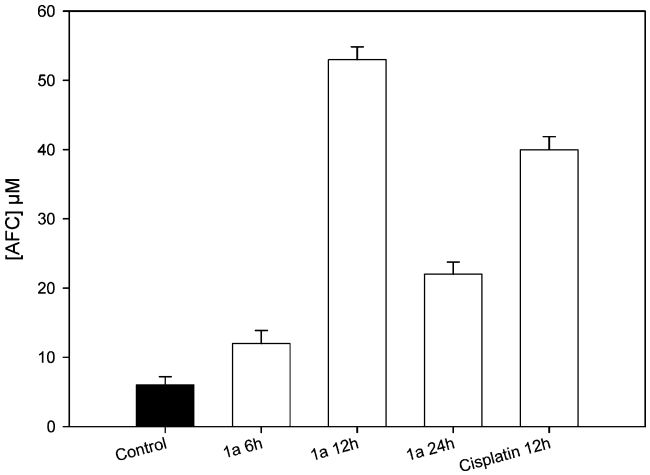

Figure 3. Induction of caspase-3. 2008 cells were incubated with IC_{50} concentrations of complex **1a** or cisplatin and then submitted to the test on caspase-3 induction as described in the Experimental Section. Data are the means of at least three independent experiments. Error bars indicate standard deviation. *$P < 0.05$ compared to untreated cells.

Inhibition of the Macromolecular Synthesis. To assess the main biological target of the new benzyliminoether complex, the macromolecular synthesis inhibition has been monitored on treated cells. DNA, RNA, and protein synthesis inhibition was evaluated in terms of tritiated thymidine, uridine, and leucine incorporation into the acid-insoluble fraction of 2008 cells, exposed for 3 h to increasing concentration of **1a**. Again, cisplatin was used as a reference compound.

Complex **1a**, regarding the inhibition of DNA synthesis (Figure 2a), promoted a strong dose-dependent decrease of ^{3}H-thymidine incorporation, reducing DNA synthesis by about 60% even at the lowest concentration (12 μM) and showing a trend very similar to that exhibited by the reference metallodrug. Regarding the ^{3}H-uridine incorporation data (Figure 2b), derivative **1a** inhibited RNA synthesis in a dose-dependent way, but with a trend very similar to that exhibited by cisplatin, that, as expected, was not very effective; in fact, it has been proven that its antitumor activity is not related to a direct inhibition of RNA synthesis.[29] With regard to protein synthesis (Figure 2c), it seemed not to be affected by treatment with cisplatin, and even the complex **1a** showed a very humble inhibitory effect.

In conclusion, the cytotoxicity of complex **1a** is mainly due to the inhibition of DNA synthesis and less to that of RNA or protein synthesis. These data agree with those previously observed in the case of the benzamidine derivative,[15] *trans*-$[PtCl_2\{N(H)=C(NMe_2)Ph\}_2]$, and suggest that derivative **1a**, as cisplatin, may interact with cellular DNA.

Induction of Apoptosis. To investigate the mechanism of cell death induced by the new benzyliminoether complex, we examined its effect on the induction of apoptosis in 2008 cells. Apoptosis is generally considered as one of the main mechanisms of the antitumor effect of cisplatin. Caspase-3 is a well-known executor enzyme in apoptosis,[30] and cisplatin may cause apoptosis associated with increased caspase-3 activity.[31] Complex **1a** was tested for its ability to induce caspases-3 activation in lysates of 2008 cells after a period of 24 h.

As shown in Figure 3, the increase of enzyme activity after cell treatment with IC_{50} concentrations of complex **1a** was time-dependent. Trials revealed that caspase-3 reached the maximum of activation after a 12 h treatment. In fact, after a 6 h incubation, only a modest increase of enzyme activity was detected, possibly because after this time the cell death pathway had not already begun, as confirmed by cytotoxicity experiments (data not shown). After a 24 h incubation, there was a lower enzyme activity than that obtained after 12 h but still higher than the control value, probably because 24 h might be too long an incubation time to point out an early event in the apoptotic cascade like the caspase activation.[32] When cells were harvested after a 12 h treatment, enzyme activation in **1a**-treated cells was about 9- and 1.3-fold higher than that detected in untreated and cisplatin-treated cells, respectively.

Albeit preliminary, this result, agreeing with cytotoxicity data, appears encouraging because it is particularly advantageous to the development of new agents able to induce tumor cell death by means of an apoptotic mechanism rather than a necrotic one.[33]

In Vivo Studies. On the basis of the in vitro studies, the most active benzyliminoether derivative **1a** was selected for *in vivo* studies. First of all, the toxicity of **1a** was assessed from the lethality in BALB/c mice within 30 days. The median lethal dose (55 mg·kg^{-1}) attests to a noticeably lower systemic toxicity than that of cisplatin (11.4 mg·kg^{-1}).

The antitumor activity of compound **1a** was evaluated, at four dose levels, in two murine tumor models, L1210 leukaemia and Lewis lung carcinoma, and compared with that of cisplatin.

To determine the therapeutic efficacy against murine leukaemia L1210, cisplatin or complex **1a** were administrated i.p. on days 1, 5, and 9 after tumor implantation. The data, expressed as a percentage value of *T*/*C* (%*T*/*C*), are summarized in Table 4.

It was found that complex **1a**, at the highest dose, significantly prolonged the life span of treated animals (%*T*/*C* = 245, $p < 0.01$), demonstrating an antitumor effect about 1.5-fold higher that that of cisplatin (%*T*/*C* = 160). Survival time of mice treated with the benzyliminoether derivative at the lowest dose was 19.71 days compared with 19.20 days in the case of treatment with cisplatin and 12.01 days of survival of the control

Table 4. In Vivo Antitumor Activity of Complex **1a** and Cisplatin in Murine L1210 Leukemia[a]

cmpd	dose[b] (mg·kg^{-1})	survival time (days ± S.D.)	%*T*/*C* [c]	body weight variation[d] (%)
control		12.01 ± 0.51		+10
1a	2.5	19.71 ± 0.43	164.1	+8
	5	21.50 ± 0.64*	179.1	+5
	7.5	26.21 ± 0.70*	218.2	+3
	10	29.50 ± 0.07**	245.6	0
cisplatin	1	19.20 ± 0.65*	159.9	−5

[a] L1210 leukaemia cells (10^5/mouse) were implanted on day 0 in BALB/c × DBA/2 F_1 mice (18 ± 2 g body weight body weight, 8 mice/group, 10 controls). [b] The treatment with tested compounds freshly dissolved in DMSO was performed i.p. on days 1, 5, and 9. [c] %*T*/*C*, mean survival time (%) of treated animals vs controls. [d] Body weight variation at the end of treatment with respect to day 0. *P < 0.05, statistical significance by Student' t-test compared to the control. **P < 0.01, statistical significance by Student' t-test compared to the control.

Table 5. In Vivo Antitumor Activity of Complex **1a** and Cisplatin in Murine L1210/R Leukemia[a]

cmpd	dose[b] (mg·kg^{-1})	survival time (days ± S.D.)	%*T*/*C*[c]	body weight variation[d] (%)
control		12.04 ± 0.43		+10
1a	2.5	20.01 ± 0.35	166.2	+7
	5	21.97 ± 0.53*	182.5	+4
	7.5	27.00 ± 0.61*	224.2	+3
	10	29.95 ± 0.04**	248.7	0
cisplatin	1	13.10 ± 0.65	108.8	−5

[a] L1210/R leukaemia cells (10^5/mouse) were implanted on day 0 in BALB/c × DBA/2 F_1 mice (18 ± 2 g body weight body weight, 8 mice/group, 10 controls). [b] The treatment with tested compounds freshly dissolved in DMSO was performed i.p. on days 1, 5, and 9. [c] %*T*/*C*, mean survival time (%) of treated animals vs controls. [d] Body weight variation at the end of treatment with respect to day 0. *P < 0.05, statistical significance by Student' t-test compared to the control. **P < 0.01, statistical significance by Student' t-test compared to the control.

Table 6. In Vivo Antitumor Activity of Complex **1a** and Cisplatin in the Murine Lewis Lung Carcinoma[a]

cmpd	dose (mg·kg^{-1})	avg tumor weight (g ± S.D.)	tumor growth inhibition (%)
control		1.025 ± 0.14	
1a	2.5	0.612 ± 0.03	40.29
	5	0.360 ± 0.01*	64.88
	7.5	0.254 ± 0.04*	75.22
	10	0.124 ± 0.02*	87.90
cisplatin	1	0.352 ± 0.05*	65.65

[a] Tumor was implanted i.m. as a 2 × 10^6 cells inoculum into the right hind leg of C57BL/6 mice (24 ± 3 g body weight, 8 animals/group, 10 controls). The treatment with tested drugs began 24 h after implant and was performed i.p. from day 1 to day 6. At day 11, the animals were sacrificed, the legs were amputated at the proximal end of the femur, and the inhibition of tumor growth was determined according to the difference in weight of the tumor-bearing leg and the healthy leg of the animals, expressed as % referred to the control animals. The body weight variation at the end of treatment with respect to day 0. *P < 0.05, statistical significance by Student' t-test compared to the control.

(untreated) group. Moreover, the treatment with complex **1a** was much less toxic toward the host; in fact, treated mice, even at the highest dose (10 mg·kg^{-1}), exerted a body weight loss significantly lower than that provoked by cisplatin.

The antileukemic activity of derivative **1a** was evaluated also in mice inoculated i.p. with L1210/R cells that acquired resistance to cisplatin in vivo[28] (see Table 5).

In L1210/R, the %*T*/*C* values obtained in mice treated with **1a** were similar to those obtained in mice implanted with L1210. On the other hand, cisplatin appeared to be almost ineffective in L1210/R bearing mice. From these data, the cisplatin resistance overcoming effect of complex **1a** has been further confirmed. The mechanism by which the lack of cross-resistance developed between cisplatin and complex **1a** are not yet clear and need to be deepened.

Chemotherapy with **1a** was performed also on Lewis lung carcinoma bearing mice i.p. from day 1 to day 6, and the tumor growth was assessed on day 11 post-implantation. The results are presented in Table 6.

Complex **1a** showed, at 5 mg·kg^{-1} dose, a significant tumor growth inhibition (64.88%), in comparison to untreated controls that appeared similar to that provoked by cisplatin. At the highest dose, instead, complex **1a** displays an antitumor activity noticeably higher (87.9% of tumor growth inhibition, $p < 0.05$), about 1.3 times, than that of the reference drug (65.65%).

All the in vivo efficacy results correlated with the data obtained in the cytotoxicity studies where compound **1a** elicited an activity markedly higher than that of cisplatin. Further studies are now in progress, aimed at establishing the efficacy profile of complex **1a** in tumor xenograft models.

In conclusion, this report reveals for the first time that an iminoether of *cis*-geometry shows a higher biological activity than the corresponding *trans*-species.

Considering the potential advantages in terms of markedly high cytotoxic activity, the overcoming of acquired and intrinsic cisplatin resistance, delineation of an apoptotic cell-death mechanism and the noticeable in vivo antitumor activity against both transplantable tumor models, **1a** represents a very interesting candidate for the development of a new class of antitumor Pt-based drugs.

Acknowledgment. This work was financially supported by University of Padua (Progetto di Ateneo CPDA065113/06) and by Ministero dell'Istruzione dell'Università e della Ricerca. We are grateful to CIRCMSB (Consorzio Interuniversitario di Ricerca in Chimica dei Metalli nei Sistemi Biologici).

Supporting Information Available: Experimental procedure and tables with structural information regarding the X-ray crystallographic analysis of **1b** in CIF format. This material is available free of charge via the Internet at http://pubs.acs.org.

References

(1) Kelland, L. R. New Platinum Drugs. In *Platinum Based Drugs in Cancer Therapy*; Kelland, L. R., Farrell, N. P., Eds.; Humana Press: Totowa, N.J., 2000; pp 299−319. (b) Lippert, B., Ed. In *Cisplatin, Chemistry and Biochemistry of a leading Anticancer Drug*; Wiley-VCH: Weinheim, 1999. (c) Wang, D.; Lippard, S. J. Cellular processing of platinum anticancer drug. *Nat. Rev. Drug Discovery* **2005**, *4*, 307−320.

(2) Wong, E.; Giandomenico, C. M. Current status of platinum-based antitumor drugs. *Chem. Rev.* **1999**, *99*, 2451−2466.

(3) Boulikas, T.; Vougiouka, M. Cisplatin and platinum drugs at the molecular level. *Oncol. Rep.* **2003**, *10*, 1663−1682.

(4) Cleare, M. J.; Hoeschele, J. D. Studies on the antitumor activity of group VIII transition metal complexes. Part I. Platinum(II) complexes. *Bioinorg. Chem.* **1973**, *2*, 187−210.

(5) Michelin, R. A.; Mozzon, M.; Bertani, R. Reactions of transition metal-coordinated nitriles. *Coord. Chem. Rev.* **1996**, *147*, 299−338.

(6) Kukushkin, V. Y.; Pombeiro, A. J. L. Additions to metal-activated organonitriles. *Chem. Rev.* **2002**, *102*, 1771−1802.

(7) Fannizzi, F. P.; Intini, F. P.; Natile, G. Nucleophilic attack of methanol on bis(benzonitrile)dichloroplatinum: formation of mono- and bis-imido ester derivatives. *J. Chem. Soc., Dalton Trans*. **1989**, 947−951.

(8) Cini, R.; Caputo, P. A.; Intini, F.P.; Natile, G. Mechanistic and stereochemical investigation of imino ethers formed by alcoholysis of coordinated nitriles: X-ray crystal structures of *cis*- and *trans*-bis(1-imino-1-methoxyethane)dichloroplatinum(II). *Inorg. Chem.* **1995**, *34*, 1130−1137.

(9) Bertani, R.; Catanese, D.; Michelin, R. A.; Mozzon, M.; Bandoli, G.; Dolmella, A. Reactions of platinum(II)−nitrile complexes with amines. Synthesis, characterization, and X-ray structure of the platinum(II)−amidine complex *trans*-[$PtCl_2${*Z*-N(H)=C(NHMe)-Me}$_2$]. *Inorg. Chem. Commun*. **2000**, *3*, 16−18.

(10) (a) Michelin, R. A.; Bertani, R.; Mozzon, M.; Sassi, A.; Benetollo, F.; Bombieri, G.; Pombeiro, A. J. L. *cis*-Addition of dimethylamine to the coordinated nitriles of *cis*- and *trans*-$[PtCl_2(NCMe)_2]$. X-ray structure of the amidine complex *cis*-$[PtCl_2\{E\text{-}N(H)=C(NMe_2)Me\}_2]\cdot CH_2Cl_2$. *Inorg. Chem. Commun*. **2001**, *4*, 275−280. (b) Belluco, U.; Benetollo, F.; Bertani, R.; Bombieri, G.; Michelin, R. A.; Mozzon, M.; Pombeiro, A. J. L.; Guedes da Silva, F. C. Stereochemical investigation of the addition of primary and secondary aliphatic amines to the nitrile complexes *cis*- and *trans*-$[PtCl_2(NCMe)_2]$. X-ray structure of the amidine complexes *trans*-$[Pt(NH_2i\text{-}Pr)_2\{Z\text{-}N(H)=C(NHi\text{-}Pr)Me\}_2]Cl_2\cdot 4H_2O$ and *trans*-$[PtCl_2(NCMe)\{E\text{-}N(H)=C(NMet\text{-}Bu)Me\}]$. *Inorg. Chim. Acta* **2002**, *330*, 229−239. (c) Belluco, U.; Benetollo, F.; Bertani, R.; Bombieri, G.; Michelin, R. A.; Mozzon M.; Tonon, O.; Pombeiro, A. J. L.; Guedes da Silva, F. C. Addition reactions of primary and secondary aliphatic amines to the benzonitrile ligands in *cis*- and *trans*-$[PtCl_2(NCPh)_2]$ complexes. X-ray structure of the amidine complex *trans*-$[PtCl_2\{Z\text{-}N(H)=C(NHt\text{-}Bu)Ph\}_2]$. *Inorg. Chim. Acta* **2002**, *334*, 437−447.

(11) (a) Natile, G.; Coluccia, M. Antitumor Active *trans*-Platinum Compounds. In *Metal Complexes in Tumor Diagnosis and as Anticancer Agents*; Sigel, A., Sigel, H., Eds.; Marcel Dekker: New York, 2004; Vol. 42 (Metal Ions in Biological Systems), pp 209−250. (b) Natile, G.; Coluccia, M. Current status of *trans*-platinum compounds in cancer therapy. *Coord. Chem. Rev.* **2001**, *216*−*217*, 383−410. (c) Coluccia, M.; Natile, G. *trans*-Platinum complexes in cancer therapy. *Anti-Cancer Agents Med. Chem.* **2007**, *7*, 111−123.

(12) Coluccia, M.; Nassi, A.; Boccarelli, A.; Giordano, D.; Cardellicchio, N.; Intini, F. P.; Natile, G.; Barletta, A.; Paradiso A. In vitro antitumor activity and cellular pharmacological properties of the platinum-iminoether complex *trans*-$[PtCl_2\{E\text{-}HN=C(OMe)Me\}_2]$. *Int. J. Oncol.* **1999**, *15*, 1039−1044. (b) Janovská, E.; Nováková, O.; Natile, G.; Brabec, V. Differential genotoxic effects of antitumor *trans*-$[PtCl_2(E\text{-iminoether})_2]$ and cisplatin in *Escherichia coli*. *J. Inorg. Biochem.* **2002**, *90*, 155−158.

(13) Brabec, V.; Vrana, O.; Novakova, A.; Kleinwachter, V.; Intini, F. P.; Coluccia, M.; Natile, G. DNA-adducts of antitumor *trans*-$[PtCl_2(E\text{-iminoether})_2]$. *Nucleic Acids Res.* **1996**, *24*, 336−341. (b) Zaludova, R.; Zakovska, A.; Kasparkova, J.; Balcarova, Z.; Vrana, O.; Coluccia, M.; Natile, G. DNA-modifications by antitumor *trans*-$[PtCl_2(E\text{-iminoether})_2]$. *Mol. Pharmacol.* **1997**, *52*, 354−361.

(14) Nováková, O.; Kasparkova, J.; Malina J.; Natile, G.; Brabec, V. DNA-protein cross-linking by *trans*-$[PtCl_2(E\text{-iminoether})_2]$. A concept for activation of the *trans*-geometry in platinum antitumor complexes. *Nucleic Acids Res.* **2003**, *31*, 6450−6460.

(15) Marzano, C.; Mazzega Sbovata, S.; Bettio, F.; Michelin, R.A.; Seraglia, R.; Kiss, T.; Venzo, A.; Bertani, R. Solution behaviour and biological activity of bis-amidine complexes of platinum(II). *J. Biol. Inorg. Chem.* **2007**, *12*, 477−493.

(16) (a) Nakamoto, K. *Infrared and Raman Spectra of Inorganic and Coordination Compounds*; John Wiley & Sons, Inc.: NY, 1986; pp 198−371. (b) Fraccarollo, D.; Bertani, R.; Mozzon, M.; Belluco, U.; Michelin, R. A. Synthesis and spectroscopic investigation of *cis*- and *trans*-isomers of bis(nitrile)dichloroplatinum(II) complexes. *Inorg. Chim. Acta* **1992**, *201*, 15−22.

(17) (a) Miller, R. G.; Stauffer, R. D.; Fahey, D. R.; Parnell, D. R. Alkenylaryl compounds of nickel(II) and palladium(II). Influence of the transition metal on ligand proton chemical shifts. *J. Am. Chem. Soc.* **1970**, *92*, 1511−1521. (b) Fahey, D. R. A very low-field aromatic proton resonance in the PMR spectrum of a conformationally constrained arylnickel complex. *J. Organomet. Chem.* **1973**, *57*, 385−388. (c) Albinati, A.; Pregosin, P. S.; Wombacher, F. Weak Pt−H−C interactions. Extensions to 8-methylquinoline, benzoquinoline, and a tetralone Schiff base. X-ray crystal structure of *trans*-$PtCl_2$(benzoquinoline)(PEt_3). *Inorg. Chem.* **1990**, *29*, 1812−1817.

(18) Berners-Price, S. J.; Appleton, T. G. The chemistry of cisplatin in aqueous solution. In *Platinum Based Drugs in Cancer Therapy*; Kelland, L.R., Farrell, N. P., Eds.; Humana Press: Totowa, N.J., 2000; pp 3−35.

(19) Geary, W. J. The use of conductivity measurements in organic solvents for the characterisation of coordination compounds. *Coord. Chem. Rev.* **1971**, *7*, 81−122.

(20) Michelin, R. A.; Mozzon, M.; Bertani, R.; Benetollo, F.; Bombieri, G.; Angelici, R. J. Reactions of aziridine with platinum(II) nitriles. Formation of (aziridino)amidines and 2-imidazolines and X-ray structure of *trans*-$[PtCl_2\{N(H)=C(\overline{NCH_2CH_2})Ph\}_2]$. *Inorg. Chim. Acta* **1994**, *222*, 327−337.

(21) Coluccia, M.; Nassi, A.; Loseto, F.; Boccarelli, A.; Mariggio, M. A.; Giordano, D.; Intini, F. P.; Caputo, P.; Natile, G. A *trans*-platinum complex showing higher antitumor activity than the *cis*-congeners. *J. Med. Chem.* **1993**, *36*, 510−512.

(22) Sergent, C.; Franco, N.; Chapusot, C.; Lizard-Nacols, S.; Isambert, N.; Correia, M.; Chauffert, B. Human colon cancer cells surviving high doses of cisplatin or oxaliplatin in vitro are not defective in DNA mismatch repair proteins. *Cancer Chemother. Pharmacol.* **2002**, *49*, 445−452.

(23) Zhang, P.; Gao, W. Y.; Turner, S.; Ducatman, B. S. Gleevec (STI-571) inhibits lung cancer cell growth (A549) and potentiates the cisplatin effect in vitro. *Mol Cancer*. **2003**, *2*, 1−9.

(24) Bocarelli, A.; Coluccia, M.; Intini, F. P.; Natile, G.; Locker, D.; Leng, M. Cytotoxicity and DNA binding mode of new platinum-iminoether derivatives with different configuration of the iminoether ligands. *Anti-Cancer Drug Des.* **1999**, *14*, 253−264.

(25) Marverti, G.; Andrews, P. A.; Piccinini, G.; Ghiaroni, S.; Barbieri, D.; Moruzzi, M. S. Modulation of *cis*-diamminedichloroplatinum-(II) accumulation and cytotoxicity by spermine in sensitive and resistant human ovarian carcinoma cells. *Eur. J. Cancer* **1997**, *33*, 669−675.

(26) Lanzi, C.; Perego, P.; Supino, R.; Romanelli, S.; Pensa, T.; Carenini, N.; Viano, I.; Colangelo, D.; Leone, R.; Apostoli, P.; Cassinelli, G.; Gambetta, R. A.; Zunino, F. Decreased drug accumulation and increased tolerance to DNA damage in tumor cells with a low level of cisplatin resistance. *Biochem. Pharmacol.* **1998**, *55*, 1247−1254.

(27) Perego, P.; Camerini, C.; Gatti, L.; Carenino, N.; Romanelli, S.; Supino, R.; Col angelo, D.; Viano, I.; Leone, R.; Spinelli, S.; Pezzoni, G.; Manzotti, C.; Farrell, N.; Zumino, F. A novel trinuclear platinum complex overcomes cisplatin resistance in an osteosarcoma cell system. *Mol. Pharmacol*. **1999**, *55*, 528−534.

(28) Tashiro, T.; Kawada, Y.; Sakurai, Y.; Kidani, Y. Antitumor activity of a new platinum complex, oxalate(trans-1−1,2-diaminocyclohexane)-platinum(II): New experimental data. *Biomed. Pharmacother.* **1989**, *43*, 251−260.

(29) Pil, P.; Lippard, S. J. Cisplatin and Related Drugs. In *Encyclopedia of Cancer*; Bertino J. R., Ed.; Academic Press: San Diego, 1997; Vol. 1, pp 392−410.

(30) Earnshaw, W. C.; Martins, L. M.; Kaufmann, S. H. Mammalian caspases: Structure, activation, substrates, and functions during apoptosis. *Annu. Rev. Biochem.* **1999**, *68*, 383−424.

(31) Henkels, K. M.; Turchi, J. J. Cisplatin-induced apoptosis proceeds by caspase-3-dependent and -independent pathways in cisplatin-resistant and -sensitive human cancer cell lines. *Cancer Res.* **1999**, *59*, 3077−3083.

(32) (a) Ishizaki, Y.; Jacobson, M. D.; Raff, M. C. A role for caspases in lens fiber differentiation. *J. Cell. Biol*. **1998**, *140*, 153−158. (b) Schotte, P.; Van Criekinge, W.; Van de Craen, M.; Van Loo, G.; Desmedt, M.; Grooten, J.; Cornelissen, M.; De Ridder, L.; Vandekerckhove, J.; Fiers, W.; Vandenabeele, P.; Beyaert, R. Cathepsin B-mediated activation of the proinflammatory caspases-11. *Biochem. Biophys. Res. Commun.* **1998**, *251*, 379−387. (c) Vancompernolle, K.; Van Herreweghe, F.; Pynaert, G.; Van de Craen, M.; De Vos, K.; Totty, N.; Sterling, A.; Fiers, W.; Vendenabeele, P.; Grooten J. Atractyloside-induced release of cathepsin B, a protease with caspases-processing activity. *FEBS Lett.* **1998**, *438*, 150−158.

(33) (a) Wyllie, A. H.; Kerr, J. F. R.; Curie, A. R. Cell death: The significance of apoptosis. In *International Review of Cytology*; Bourne, G. H., Danielli, F. J., Jeon, K.W., Eds.; Academic Press: New York, 1980; Vol. 68, pp 251−306. (b) Pérez, J. M.; Fuertes, M. A.; Alonso, C.; Navarro-Ranninger, C. Current status of the development of *trans*-platinum antitumor drugs. *Crit. Rev. Oncol./Hematol.* **2000**, *35*, 109−120. (c) Khazanow, E.; Barenholz, Y.; Gibson, D.; Najajreh, Y. Novel apoptosis-inducing *trans*-platinum piperidine derivatives: Synthesis and biological characterization. *J. Med. Chem*. **2002**, *45*, 5196−5204.

(34) (a) Bax, A.; Subramian, S. Sensitivity-enhanced two-dimensional heteronuclear shift correlation NMR spectroscopy. *J. Magn. Reson*. **1986**, *67*, 565−569. (b) Drobny, G.; Pines, A.; Sinton, S.; Weitekamp, D. P.; Wemmer, D. Fourier transform multiple quantum nuclear magnetic resonance. *Faraday Symp. Chem. Soc*. **1978**, *13*, 49−55.

(35) (a) Otting, G.; Wüthrich, K. Efficient purging scheme for proton-detected heteronuclear two-dimensional NMR. *J. Magn. Reson*. **1988**, *76*, 569−574. (b) Bax, A.; Summers, M. F. ^1H and ^{13}C assignments from sensitivity-enhanced detection of heteronuclear multiple-bond connectivity by 2D multiple quantum NMR. *J. Am. Chem. Soc*. **1986**, *108*, 2093−2094.

(36) Kauffmann, G. B.; Cowan, D. O. *cis*- and *trans*-Dichlorodiammine-platinum(II). In *Inorganic Syntheses*; Kleinberg, J., Ed.; McGraw-Hill Book Company: New York, 1963; Vol. VII, pp 239−245.

(37) Kukushkin, V.Y.; Tkachuk, V.M. Synthesis, thermal isomerization in solution and in solid phase of the complexes $[Pt(RCN)_2Cl_2]$. *Z. Anorg. Allg. Chem.* **1992**, *613*, 123−126.

(38) Atkins, P. W. *Physical Chemistry*; Oxford University Press: Oxford, 1998.

(39) North, A. T. C.; Philips, D. C.; Mathews, F. S. A semi-empirical method for absorption correction. *Acta Crystallogr*. **1968**, *A24*, 351−359.

(40) Sheldrick, G. M. "SHELXS-86", program for crystal structures determination. *Acta Crystallogr*. **1990**, *A46*, 467−473.
(41) Sheldrick, G. M. *SHELXL-97*, program for the refinement of crystal structures; University of Göttingen: Germany, 1997.
(42) Farrugia, L. J. WinGX suite for small-molecule single-crystal crystallography. *J. Appl. Crystallogr*. **1999**, *32*, 837−388.
(43) Alley, M. C.; Scudiero, D. A.; Monks, A.; Hursey, M. L.; Czerwinski, M. J.; Fine, D. L.; Abbott, B. J.; Mayo, J. G.; Shoemaker, R. H.; Boyd, M. R. Feasibility of drug screening with panels of human tumor cell lines using a microculture tetrazolium assay. *Cancer Res.* **1988**, *48*, 589−601.

JM070426P